Effect of manganese doping on optical and magnetic properties of titanium dioxide nanostructures prepared by hydrothermal technique in the presence of thiourea

Golnoush Zamiri[1], Azmi Zakaria[1], Mohd Zobir Hussein[2], Reza Zamiri[3], Avito Rebelo[3], Hossein Abbastabar Ahangar[4]

[1]*Department of Physics, Faculty of Science, University Putra Malaysia, 43400 UPM Serdang, Selangor, Malaysia*
[2]*Department of Chemistry, Faculty of Science, University Putra Malaysia, 43400 UPM Serdang, Selangor, Malaysia*
[3]*Department of Materials Engineering and Ceramic, CICECO, University of Aveiro, Campus Santiago, 3810–193 Aveiro, Portugal*
[4]*Faculty of Chemistry, Kharazmi (Tarbiat Moallem) University, Tehran, Iran*
E-mail: azmizak@gmail.com

Published in Micro & Nano Letters; Received on 5th March 2014; Revised on 12th August 2014; Accepted on 19th August 2014

Manganese (Mn)-doped titanium dioxide (TiO_2) nanostructures were synthesised by hydrothermal reaction of TiO_2 and Mn acetate with ethylenediamine and thiourea. The prepared samples were characterised by X-ray diffraction, Fourier transform infrared spectroscopy, transmission electron microscopy, field emission scanning electron microscopy and energy dispersive X-ray spectroscopy. Characterisation of samples confirmed the formation of pure and crystalline nanostructures. Photoluminescence spectroscopy was carried out to study the optical properties of the pure and Mn-doped TiO_2 nanostructures. A vibrating sample magnetometer was used to study the magnetic properties of the prepared Mn-doped TiO_2 nanostructures.

1. Introduction: The titanium dioxide (TiO_2) nanostructure is an important semiconductor material with good photo-catalytic properties and non-toxicity. It has been extensively used in different fields of application, such as addressing environmental problems as a photo-catalyst, in cancer treatment [1], photonic crystals [2], UV blockers [3], self-cleaning materials [4] and in dye-sensitised solar cells [5]. These applications originated from the specific ionic and electronic properties of TiO_2, which depend on the particular crystal structure (anatase, rutile or brookite) and its morphology as well as bandgap energy. The TiO_2 nanostructure bandgap energy is much higher than that of bulk TiO_2 [6]. The bandgap of the anatase form is 3.20 eV with the absorption edge in the near UV area at 386 nm [7]. The occurrence of an electron excitation from the valence band to the conduction band originates a hole in the valence band whenever a semiconductor is illuminated by light of energy higher than its bandgap. TiO_2 can be excited by UV light because of its wide bandgap (3.2 eV for anatase phase). The practical applications of TiO_2 are limited in most conditions because of its wide gap. The bandgaps of TiO_2 can be narrowed by doping the compounds with metal (such as Fe, Cr, Co, Mn, V and Ni) or non-metal atoms. Manganese (Mn) has the highest potential in permitting important optical absorption in the visible or even the infrared solar light between the 3d metals as theoretical modelling has shown. The optical absorption energy of TiO_2 is increased from the limited ultraviolet spectral range well into the major visible and even infrared range by doping Mn with TiO_2 [8, 9]. Mn may be considered a magnetic material that behaves as a soft ferromagnetic material. Soft ferromagnetic or ferrimagnetic materials have important properties such as high permeability, high saturation induction and low coercive force. Technical applications were developed using soft ferromagnetic materials to allow changes in magnetisation to occur easily in weak magnetic fields. There are several techniques to prepare Mn-doped TiO_2 nanostructures including vapour–solid growth or vapour–liquid–solid techniques [10], and methods employing templates such as lyotropic liquid crystals [11] or porous aluminium oxides [12]. Special equipment and high temperatures are required to prepare Mn-doped TiO_2 nanostructures by vapour methods. Prefabrication and post-removal of the templates commonly produces contaminations, which is a frequent problem of the template technique. Nowadays, a considerable number of studies have pointed to the hydrothermal technique as a powerful and encouraging method for preparing one-dimensional (1D) nanomaterials, such as nanowires and nanotubes. Since it is a simple procedure and of low cost, it can be worthwhile to use hydrothermal reactions for the synthesis of nanostructures [13]. Obviously, hydrothermal treatment can control the morphology of the nanostructures by changing the structure (or size) of raw materials, reaction temperature and time and the concentration and species of the alkaline solution [14]. In this Letter, we study the optical and magnetic properties of Mn-doped TiO_2 nanostructures prepared through hydrothermal reaction of Mn and TiO_2 in the presence of ethylenediamine (EN) and thiourea (TN) as capping agents.

2. Methodology: A 9 mol% Mn-doped TiO_2 nanostructure was prepared by mixing 10 mmol of TiO_2, 0.9 mmol of Mn, 15 mmol of EN, 13 mmol of TH and 40 ml of distilled water. The solution was transferred to a teflon-lined autoclave of 60 ml capacity and heated at 130°C for 6 h and then allowed to cool down to room temperature naturally. A light brown precipitate was collected and washed several times with ethanol and distilled water, and after that was dried in an oven at 75°C for a few hours.

X-ray diffraction (XRD) signals and Fourier transform infrared spectroscopy (FTIR) spectra were recorded with a Shimadzu XRD-6000 X-ray diffractometer (Shimadzu, Tokyo, Japan) and a Perkin Elmer 1650 FTIR spectrometer (Perkin Elmer, Waltham, MA, USA), respectively. Morphological evaluation was performed with a Hitachi H-7100 transmission electron microscope (TEM; Hitachi, Chula Vista, CA, USA) operating at an accelerating voltage of 120 kV and a field emission scanning electron microscope (FESEM) (model: Nova Nanosem 230). Photoluminescence (PL) spectroscopy was carried out by a fluorescence spectrometer (Perkin-Elmer LS55).

3. Results and discussion: Fig. 1 shows the XRD patterns of pure and Mn-doped TiO_2 nanostructures. It was found that the diffraction peaks of TiO_2 well agree with a standard anatase of TiO_2 (JCPDS 21-1272) [15]. The crystal structure of the

doi: 10.1049/mnl.2014.0120

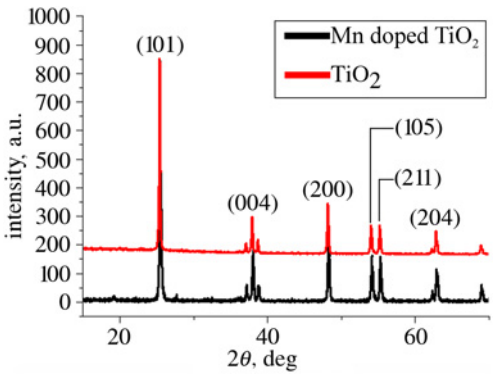

Figure 1 *XRD pattern of TiO_2 and Mn-doped TiO_2 nanostructures*

Table 1 Crystallite size and vertical distance of crystal planes

Sample	FWHM (rad × 10^{-3})	*D*, nm	*d*, nm
1	2.963394	35.15	0.35
2	3.99942	47.42	0.35

Mn-doped sample has the same diffraction peaks as the sample of TiO_2, as it has a similar inter-layer spacing of 0.35 nm (see Table 1). On the other hand, there are no appearing peaks related to manganese oxide impurity phase formation.

Table 1 summarises the vertical distance between pairs of adjacent planes in the crystals (d), which was calculated using Bragg's law by the following equation

$$n\lambda = 2d \sin \theta \tag{1}$$

where θ is the angle, n is the layer of planes and λ is the wavelength of the X-rays; the crystallite size was estimated from the Debye-Scherrer formula by the following equation

$$D = \frac{k\lambda}{\beta \cos \theta} \tag{2}$$

where D is the crystallite size, λ is the X-ray wavelength (Cu Kα = 0.15405980 nm), k is a constant taken as 0.94, θ is the peak position and β is the line broadening at the full width at half the maximum (FWHM) height. As shown in Table 1, the crystallite size of the TiO_2 nanostructures (sample 2) decreased from 47 to 35 nm after Mn doping (sample 1).

For comparison purposes the FESEM images of Mn-doped TiO_2 and pure TiO_2 are shown in Fig. 2. It can be seen that the morphology of a pure TiO_2 nanostructure sample shifts from a nanorod and nanoparticle shape to a flower-like shape after Mn doping. This change in morphology might be attributed to the lower growth rate along the {001} direction in the Mn-doped TiO_2 nanostructure,

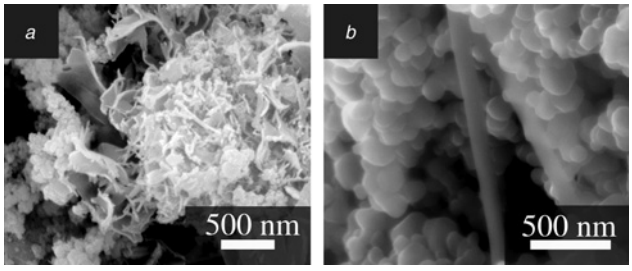

Figure 2 *FESEM image of Mn-doped and undoped TiO_2 nanostructures*
a Mn-doped TiO_2
b Undoped TiO_2

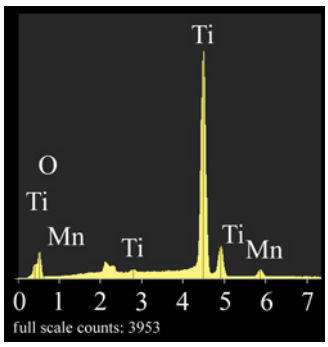

Figure 3 *EDX analysis of the prepared Mn-doped TiO_2 nanstructure*

facilitating crystalline growth in both the {100} and the {101} directions with lower surface energy [16, 17]. The EDX analysis of the Mn-doped TiO_2 nanostructure is indicated in Fig. 3 and confirms that the sample is composed of Mn, Ti and O. The absence of extra peaks besides the expected ones suggests that the obtained products are very pure.

Fig. 4 shows the FTIR spectra for Mn-doped TiO_2 and undoped TiO_2. It can be seen that in the Mn-doped TiO_2 and TiO_2 nanostructures the characteristic band is positioned at 650 cm^{-1} because of TiO_2 and assigned to the stretching of Ti–O–Ti. The characteristic peak at 1090 cm^{-1} is attributed to the stretching of O–O. The absorption band at 1390 cm^{-1} can be corresponding to the lattice vibrations of TiO_2. The peak at 1420 cm^{-1} may be assigned to C–N stretching in TH. The absorption band at 1620 cm^{-1} is because of a bending vibration of the coordinated H_2O as well as Ti–OH, and also the characteristic band position at 3394 cm^{-1} is attributed to O–H stretching. The absorption band at 1650 cm^{-1} (NH_2 bending mode) indicates absorption of TH and/or EN on the surface of the TiO_2 nanostructures. In addition, the characteristic peak at 947 cm^{-1} corresponds to Mn–O stretching [18–21].

The PL spectra of the undoped and the Mn-doped TiO_2 nanostructure at an excitation wavelength of 227 nm are presented in Fig. 5. The maximum peak is at 384 nm for the Mn-doped TiO_2 nanostructure and at 383 nm for the undoped TiO_2 nanostructure. The bandgap energies of the samples corresponding with these wavelengths were calculated by the following equation

$$\text{Bandgap} = \frac{hc}{\lambda_{\text{bandgap}}} \tag{3}$$

where h is the Plank constant (6.626×10^{-34} JS), c is the speed of light (3.0×10^{8} m/s) and λ is the wavelength.

The obtained bandgaps of the Mn-doped and undoped TiO_2 are 3.23 and 3.24 eV, respectively. Therefore the bandgap energy of the undoped TiO_2 sample is almost similar to the Mn-doped TiO_2

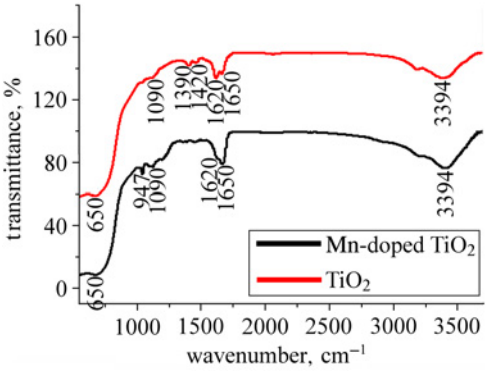

Figure 4 *FTIR spectra of Mn-doped and undoped TiO_2 nanostructures*

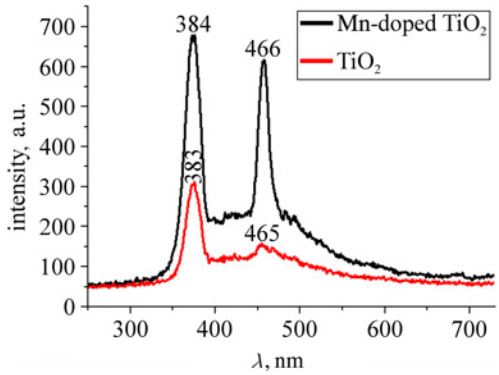

Figure 5 *PL spectra of undoped and Mn-doped TiO_2 nanostructures*

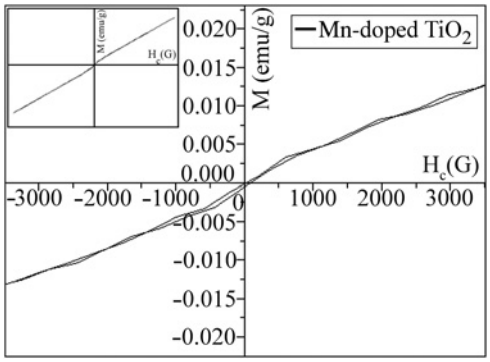

Figure 6 *VSM analysis of Mn-doped TiO_2 nanostructure*

nanostructure because of the low amount of Mn doping, which is contrary to the literature results [9, 10]. The sharp peak at 466 nm is attributed to oxygen defects in TiO_2 [22] and it became sharper after Mn doping. Therefore the oxygen defects in TiO_2 were increased because of Mn doping.

Fig. 6 shows clear hysteresis loops in the prepared Mn-doped TiO_2 nanostructure. The obtained ferromagnetic behaviour is consistent with previous reports for anatase [23] and rutile [24] Mn-doped TiO_2 which was explained within the scope of the bound magnetic polaron theory [25]. The coercivity (H_c), magnetisation and retentivity of the sample which was measured by the vibrating sample magnetometer (VSM) are 29.496 G, 47.031×10^{-2} and 190.76×10^{-6} emu/g, respectively. Materials with low coercivity are soft ferromagnetic materials and, therefore, Mn-doped TiO_2 is a soft ferromagnetic material. A similar weak hysteresis was also obtained by Peng *et al.* [26] with a similar sample prepared by the sol–gel process.

4. Conclusion: Mn-doped TiO_2 nanostructures have been successfully prepared by the hydrothermal method in the presence of EN and TH as directing agents. The effect of Mn dopants on the optical and magentical properties of the prepared samples has been studied. It was found that the bandgap of the prepared undoped and Mn-doped TiO_2 nanostructures is almost the same. The PL spectra showed a sharp peak at 466 nm because of oxygen defects in TiO_2 and it became sharper by Mn doping. The VSM result showed ferromagnetism in the sample and confirmed that the prepared nanostructure is a soft ferromagnetic material.

5. Acknowledgments: The authors thank the Ministry of Higher Education Malaysia for funding this project under the Research University Grant Scheme (RUGS) of Project No. 05-02-12-1878RU and for the grant for External Collaborative Research SFRH/BPD/76185/2011 (R.Z).

6 References

[1] Hayashi K., Nakamura M., Makita Y., Fujiwara R., Kori T., Ishimura K.: 'Synthesis and photocatalytic activity of sea urchin-shaped rutile TiO_2 nanocrystals', *Mater. Lett.*, 2011, **65**, pp. 3037–3040

[2] Wijnhoven J., Vos W.L.: 'Preparation of photonic crystals made of air spheres in titania', *Science*, 1998, **281**, pp. 802–804

[3] Viana M.M., Soares V.F., Mohallem N.D.S.: 'Synthesis and characterization of TiO_2 nanoparticles', *Ceram. Int.*, 2010, **36**, pp. 2047–2053

[4] Yuranova T., Mosteo R., Bandara J., Laub D., Kiwi J.: 'Self-cleaning cotton textiles surfaces modified by photoactive SiO_2/TiO_2 coating', *J. Mol. Catal. A, Chem.*, 2006, **244**, pp. 160–167

[5] Peining Z., Nair A.S., Shengyuan Y., Ramakrishna S.: 'TiO_2–MWCNT rice grain-shaped nanocomposites: synthesis, characterization and photocatalysis', *Mater. Res. Bull.*, 2011, **46**, pp. 588–595

[6] Bauer S., Pittrof A., Tsuchiya H., Schmuki P.: 'Size-effects in TiO_2 nanotubes: diameter dependent anatase/rutile stabilization', *Electrochem. Commun.*, 2011, **13**, pp. 538–541

[7] Banerji S., Sardar M., Tyagi A.K., Raj B.: 'Physics and chemistry of photocatalytic titanium dioxide: visualization of bactericidal activity using atomic force microscopy', *Curr. Sci.*, 2006, **90**

[8] Deng Q.R., Xia X.H., Guo M.L., Gao Y., Shao G.: 'Mn-doped TiO_2 nanopowders with remarkable visible light photocatalytic activity', *Mater. Lett.*, 2011, **65**, pp. 2051–2054

[9] Yahya K.: 'Characterization of pure and dopant TiO_2 thin films for gas sensors applications'. PhD thesis, University of Technology, Baghdad, 2010

[10] Jung W.S.: 'Preparation of gallium nitride powders and nanowires from a gallium (iii) nitrate salt in flowing ammonia', *Bull. Korean Chem. Soc.*, 2004, **25**, pp. 51–54

[11] Park I.S., Jang S.R., Hong J.S., Vittal R., Kim K.J.: 'Preparation of composite anatase TiO_2 nanostructure by precipitation from hydrolyzed $TiCl_4$ solution using anodic alumina membrane', *J. Mater. Chem.*, 2003, **15**, pp. 4633–4636

[12] Zhang Y., Li G., Wu Y., Zhang B., Song W., Zhang L.: 'Antimony nanowire arrays fabricated by pulsed electrodeposition in anodic alumina membranes', *Adv. Mater.*, 2004, **14**, pp. 1227–1230

[13] Zhao Y., Jin J., Yang X.: 'Hydrothermal synthesis of titanate nanowire arrays', *Mater. Lett.*, 2007, **61**, pp. 384–388

[14] Jitputti J., Suzuki Y., Yoshikawa S.: 'Synthesis of TiO_2 nanowires and their photocatalytic activity for hydrogen evolution', *Catal. Commun.*, 2008, **9**, pp. 1265–1271

[15] Smith L., Kuncic Z., Ostrikov K.K., Kumar S.: 'Nanoparticles in cancer imaging and therapy', *J. Nanomater.*, 2012, pp. 1–7

[16] Wu G., Wang J., Thomas D.F., Chen A.: 'Synthesis of F-doped flower-like TiO_2 nanostructures with high photoelectro chemical activity', *Langmuir*, 2008, **24**, pp. 3503–3509

[17] Gao M., Xu Y., Bai Y., Xiao F.: 'Nb, F-codoped TiO_2 hollow spheres with high visible light photocatalytic activity', *Nanoscale Res. Lett.*, 2013, **8**, p. 508

[18] Ezema F., Nwankwo U.: 'Effect of concentration of Mn dopant ions on the structural and optical properties of zinc oxide crystals', *J. Nanomater. Biostruct.*, 2011, **6**, pp. 271–278

[19] Mali S.S., Shinde P.S., Betty C.A., Bhosale P.N., Lee W.J., Patil P.S.: 'Nanocoral architecture of TiO_2 by hydrothermal process: synthesis and characterization', *Appl. Surf. Sci.*, 2011, **257**, pp. 9737–9746

[20] Zamiri R., Zakaria A., Ahangar H.A., Zamir G., Bahari H.R., Drummen G.: 'Hydrothermal synthesis of Goethite (α-FeOOH) nanorods in the presence of ethylenediamine: thiourea', *J. Nanoparticle Res.*, 2014

[21] Yuan Z., Su B.: 'Titanium oxide nanotubes, nanofibers and nanowires', *Colloids Surf. A, Physicochem. Eng. Aspects*, 2004, **241**, pp. 173–183

[22] Li H., Liu M., Zeng Y., Huang T.: 'Coexistence of antiferromagnetic and ferromagnetic in Mn-doped anatase TiO_2 nanowires', *J. Central South Univ. Technol.*, 2010, **17**, pp. 239–243

[23] Bhattacharyya S., Pucci A., Zitoun D.: 'One-pot fabrication and magnetic studies of Mn-doped TiO_2 nanocrystals with an encapsulating carbon layer', *Nanotechnology*, 2008, **19**, p. 495711

[24] Kim K., Park Y., Lee J., *ET AL.*: *J. Magn. Magn. Mater.*, 2007, **316**, p. 215

[25] Coey J.M.D., Venkatesan M., Fitzgerald C.B.: 'Donor impurity band exchange in dilute ferromagnetic oxides', *Nature Mater.*, 2005, **4**, p. 173

[26] Peng D., Fa-Min L., Chuang-Cang Z., *ET AL.*: 'Structure, room-temperature magnetic and optical properties of Mn-doped TiO_2 nano powders prepared by the sol–gel process', *Chin. Phys.*, 2010, 19, p. 118102

doi: 10.1049/mnl.2014.0120